Brain Mapping with the Ricci Flow Conformal Parameterization and Multivariate Statistics on Deformation Tensors

Yalin Wang[1,2], Xiaotian Yin[3], Jie Zhang[4], Xianfeng Gu[3], Tony F. Chan[2], Paul M. Thompson[1], and Shing-Tung Yau[5]

[1] Lab. of Neuro Imaging, UCLA School of Medicine, Los Angeles, CA 90095, USA,
[2] Mathematics Department, UCLA, Los Angeles, CA 90095, USA,
[3] Computer Science Dept., SUNY at Stony Brook, Stony Brook, NY 11794, USA,
[4] Mathematics Department, Zhejiang University, Hangzhou, China
[5] Department of Mathematics, Harvard University, Cambridge, MA 02138, USA,
{ylwang}@math.ucla.edu

Abstract. By solving the Yamabe equation with the discrete surface Ricci flow method, we can conformally parameterize a multiple boundary surface by a multi-hole disk. The resulting parameterizations do not have any singularities and they are intrinsic and stable. For applications in brain mapping research, first, we convert a cortical surface model into a multiple boundary surface by cutting along selected anatomical landmark curves. Secondly, we conformally parameterize each cortical surface using a multi-hole disk. Inter-subject cortical surface matching is performed by solving a constrained harmonic map in the canonical parameter domain. To map group differences in cortical morphometry, we then compute a manifold version of Hotelling's T^2 test on the Jacobian matrices. Permutation testing was used to estimate statistical significance. We studied brain morphology in 21 patients with Williams Syndrome (WE) and 21 matched healthy control subjects with the proposed method. The results demonstrate our algorithm's potential power to effectively detect group differences on cortical surfaces.

1 Introduction

Surface-based modeling is valuable in brain imaging to help analyze anatomical shape, to detect abnormalities of cortical surface folding, and to statistically combine or compare 3D anatomical models across subjects. Even so, a direct mapping between two 3D surfaces from different subjects is challenging to compute. Often, higher order correspondences must be enforced between specific anatomical points, curved landmarks, or subregions lying within the two surfaces. This is often achieved by first mapping each of the 3D surfaces to canonical parameter spaces such as a sphere [1, 2] or a planar domain [3]. A flow, computed in the parameter space of the two surfaces [4, 5], then induces a correspondence field in 3D. This flow can be constrained using anatomic landmark points or curves, by constraining the mapping of surface regions represented implicitly using level

sets [3], or by using currents to represent anatomical variation [6] Feature correspondence between two surfaces can be optimized by using the L^2-norm to measure differences in curvature profiles or convexity [1] or by using mutual information to align scalar fields of various differential geometric parameters defined on the surface [7]. Artificial neural networks may also be used to rule out or favor certain types of feature matches [8]. Finally, correspondences may be determined by using a minimum description length (MDL) principle, based on the compactness of the covariance of the resulting shape model [9]. Anatomically homologous points can then be forced to match across a dataset. Thodberg [10] identified problems with early MDL approaches and extended them to an MDL appearance model, when performing unsupervised image segmentation.

All oriented surfaces have conformal structures. The conformal structure is, in some respects, more flexible than the Riemannian metric but places more restrictions on the the surface morphology than the topological structure. The Ricci flow method can conformally map an open boundary surface to a multi-hole disk [11]. Compared with other conformal parameterization methods [12–15], the Ricci flow method can handle cortical surfaces with complicated topologies without singularities. The continuous Ricci flow conformally deforms a Riemannian metric on a smooth surface such that the Gaussian curvature evolves like a heat diffusion process. In the discrete case, with the circle packing metric, the Ricci flow can be formulated in a variational setting and solved by the Newton method [11].

Tensor-based morphometry is widely used in computational anatomy as a means to understand shape variation between structural brain images. Techniques based on Riemannian manifolds to compare deformation tensors or strain matrices were introduced in [16–18]. In [19], the full deformation tensors were used in the context of tensor-based morphometry. In a conformal parameterization, the original metric tensor is preserved up to a constant. The conformal parametrization provides an ideal framework to apply tensor based morphometry on surfaces, to help understand shape variation between structural brain images.

In this paper, we use the Ricci flow method to compute a conformal mapping between cortical surfaces and a multi-hole surface. Then we compute a direct cortical surface correspondence by computing a constrained harmonic map on the parameter domain. We apply multivariate statistics to the Jacobian matrices to study cortical surface variation between a group of patients with Williams syndrome (WS) and a group of healthy control subjects. WS is a genetic disorder in which the cortex develops abnormally, but the scope and type of systematic differences is unknown [20]. In our experimental results, we identified several significantly different areas on the left and right cortical surfaces between WS patients and control subjects.

2 Ricci Flow Conformal Parameterization

In this section, we introduce the theory of Ricci flow in the continuous setting, and then generalize it to the discrete setting.

2.1 Ricci Flow on Continuous Surfaces

Riemannian Metric and Gaussian Curvature All the concepts used here may be found, with detailed explanations, in [21]. Suppose S is a C^2 smooth surface embedded in $\mathbb{R}^3$ with local parameters (u_1, u_2). Let $\mathbf{r}(u_1, u_2)$ be a point on S and $d\mathbf{r} = \mathbf{r}_1 du_1 + \mathbf{r}_2 du_2$ be the tangent vector defined at that point, where $\mathbf{r}_1, \mathbf{r}_2$ are the partial derivatives of $\mathbf{r}$ with respect to u_1 and u_2, respectively. The *Riemannian metric* or the *first fundamental form* is:

$$< d\mathbf{r}, d\mathbf{r} >= \sum < \mathbf{r}_i, \mathbf{r}_j > du_i du_j, \quad i, j = 1, 2. \tag{1}$$

The Gauss map $G : S \to \mathbb{S}^2$ from the surface S to the unit sphere $\mathbb{S}^2$ maps each point p on the surface to its normal $\mathbf{n}(p)$. The *Gaussian curvature* $K(p)$ *is defined as the Jacobian of the Gauss map*. Intuitively, it is the ratio between the infinitesimal area of the image of the Gauss map and the infinitesimal area on the original surface.

The total curvature of a compact surface is determined by the topology of the surface: $\int_S K dA + \int_{\partial S} k_g ds = 2\pi\chi(S)$, where ∂S is the boundary of the surface S, k_g is the geodesic curvature, and $\chi(S)$ is the Euler characteristic of the surface (an integer).

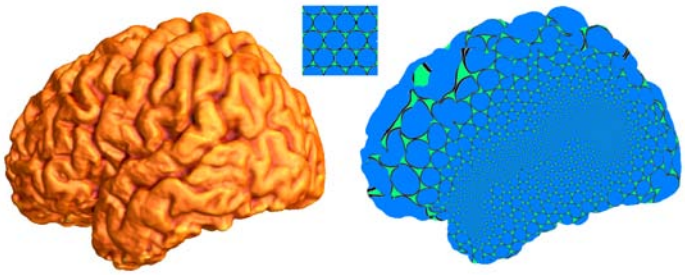

Fig. 1. Properties of Conformal Mapping: Conformal mappings transform infinitesimal circles to infinitesimal circles and preserve the intersection angles among the circles. Here, infinitesimal circles are approximated by finite ones.

Conformal deformation Let S be a surface embedded in $\mathbb{R}^3$. S has a Riemannian metric induced from the Euclidean metric of $\mathbb{R}^3$, denoted by $\mathbf{g}$. Suppose $u : S \to \mathbb{R}$ is a scalar function defined on S. It can be verified that $\bar{\mathbf{g}} = e^{2u}\mathbf{g}$ is also a Riemannian metric on S, and angles measured by $\mathbf{g}$ are equal to those measured by $\bar{\mathbf{g}}$. We say $\bar{\mathbf{g}}$ is a *conformal deformation* from $\mathbf{g}$. Figure

1 shows that a conformal deformation maps infinitesimal circles to infinitesimal circles and preserves their intersection angles.

When the Riemannian metric is conformally deformed, curvatures will also be changed accordingly. Suppose $\mathbf{g}$ is changed to $\bar{\mathbf{g}} = e^{2u}\mathbf{g}$, the Gaussian curvature will become $\bar{K} = e^{-2u}(-\Delta_{\mathbf{g}}u + K)$, where $\Delta_{\mathbf{g}}$ is the Laplacian-Beltrami operator under the original metric $\mathbf{g}$. The geodesic curvature will become $\bar{k} = e^{-u}(\partial_{\mathbf{r}}u + k)$, where $\mathbf{r}$ is the tangent vector orthogonal to the boundary.

Smooth Surface Ricci Flow Suppose S is a smooth surface with a Riemannian metric $\mathbf{g}$. The Ricci flow deforms the metric $\mathbf{g}(t)$ according to the Gaussian curvature $K(t)$ (induced by $\mathbf{g}(t)$ itself), where t is the time parameter

$$\frac{dg_{ij}(t)}{dt} = -2K(t)g_{ij}(t). \tag{2}$$

If we replace the metric in Eq. 2 with $g(t) = e^{2u(t)}g(0)$, then the Ricci flow can be simplified as $du(t)/dt = -2K(t)$, which states that the metric should change according to the curvature.

The Ricci flow can be easily modified to compute a metric with a *user-defined* curvature $\bar{K}$: $du(t)/dt = 2(\bar{K} - K)$. The resulting metric $\mathbf{g}(\infty)$ will induce the user-defined curvature $\bar{K}$.

The Ricci flow has been proven to converge. For surfaces with non-positive and positive Euler numbers, the proofs were given by Hamilton [22] and Chow [23] respectively. For a closed surface, if the total area is preserved during the flow, the Ricci flow will converge to a metric such that the Gaussian curvature is constant everywhere.

2.2 Ricci Flow on Discrete Surfaces

In engineering fields, smooth surfaces are often approximated by simplicial complexes (triangle meshes). Key concepts, such as the metric, curvature, and conformal deformation in the continuous setting can be generalized to the discrete setting. We denote a triangle mesh as Σ, the mesh boundary as $\partial\Sigma$, a vertex set as V, an edge set as E, and a face set as F. e_{ij} represents the edge connecting vertices v_i and v_j, and f_{ijk} denotes the face formed by v_i, v_j, and v_k.

Discrete Riemannian Metric and Gaussian Curvature A Riemannian metric on a mesh Σ is a piecewise constant metric with cone singularities at vertices.

The edge lengths of a mesh Σ are sufficient to define the Riemannian metric, $l : E \to \mathbb{R}^+$, as long as for each face f_{ijk}, the edge lengths satisfy the triangle inequality: $l_{ij} + l_{jk} > l_{ki}$.

The discrete Gaussian curvature K_i on a vertex $v_i \in \Sigma$ can be computed from the angle deficit,

$$K_i = \begin{cases} 2\pi - \sum_{f_{ijk}\in F} \theta_i^{jk}, & v_i \notin \partial\Sigma \\ \pi - \sum_{f_{ijk}\in F} \theta_i^{jk}, & v_i \in \partial\Sigma \end{cases} \tag{3}$$

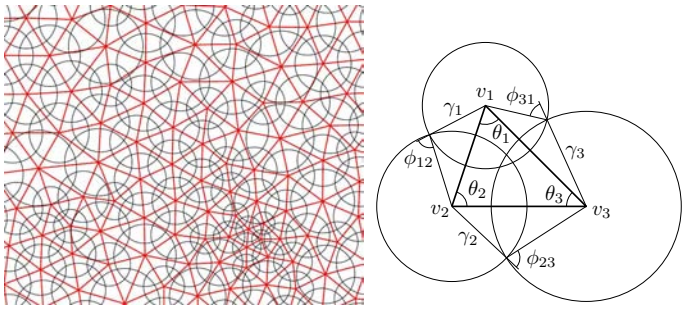

(a) (b)

Fig. 2. Circle Packing Metric (a) Flat circle packing metric (b) Circle packing metric on a triangle.

where θ_i^{jk} represents the corner angle attached to vertex v_i in the face f_{ijk}. The discrete Gaussian curvatures are determined by the discrete metrics. And the total discrete curvature is, similar to the smooth case, a topological invariant: $\sum_{v_i \in V} K_i = 2\pi\chi(M)$.

Discrete Conformal Deformation In the discrete setting, conformal deformation is carried out using the concept of *circle packing metric*, which was introduced by Thurston in [24].

By approximating infinitesimal circles using circles with finite radii, a *circle packing metric* of Σ can be denoted as (Γ, Φ), where Γ is a vertex function, $\Gamma : V \to \mathbb{R}^+$, which assigns a radius γ_i to the vertex v_i; Φ is an edge weight function, $\Phi : E \to [0, \frac{\pi}{2}]$, which assigns an acute angle (i.e. weight) $\Phi(e_{ij})$ to each edge e_{ij}. Figure 2 illustrates the circle packing metric. Each vertex v_i has a circle whose radius is γ_i. For each edge e_{ij}, the intersection angle ϕ_{ij} is defined through two circles around v_i and v_j, which either intersect or are tangent.

Two circle packing metrics (Γ_1, Φ_1) and (Γ_2, Φ_2) on the same mesh are *conformally equivalent* if $\Phi_1 \equiv \Phi_2$. A *conformal deformation* of a circle packing metric only modifies the vertex radii and preserves the intersection angles of the edges.

Discrete Surface Ricci Flow Suppose (Σ, Φ) is a weighted mesh with an initial circle packing metric. Similar to the smooth setting, if we set $\bar{\mathbf{k}} = (\bar{K}_1, \bar{K}_2, \cdots, \bar{K}_n)^T$ to be the user-defined target curvature, the discrete Ricci flow can be defined as :

$$\frac{du_i(t)}{dt} = (\bar{K}_i - K_i), \tag{4}$$

The Discrete Ricci flow can be formulated in the variational setting; namely, it is a negative gradient flow of a special energy form. Let (Σ, Φ) be a weighted mesh with spherical (Euclidean or hyperbolic) background geometry. For arbitrary two vertices v_i and v_j, the following symmetric relation holds: $\partial K_i / \partial u_j = \partial K_j / \partial u_i$. Let $\omega = \sum_{i=1}^n K_i du_i$ be a differential one-form [25]; the symmetric relation guarantees that this one-form is closed (curl free) in the metric space:

$d\omega = 0$. Then by Stokes theorem, the following integration is path independent:

$$f(\mathbf{u}) = \int_{\mathbf{u_0}}^{\mathbf{u}} \sum_{i=1}^{n} (\bar{K}_i - K_i) du_i, \tag{5}$$

where n is the number of vertices, $\mathbf{u_i} = \log(\gamma_i)$, γ_i is the radius associated with edge i, and $\mathbf{u_0}$ is an arbitrary initial metric.

The above integration (Eq. 5) is called the *discrete Ricci energy*, which is well-defined. The discrete Ricci energy has been proved to be strictly convex (i.e., its Hessian is positive definite) in [26]. The global minimum uniquely exists, which gives the desired discrete metric that induces $\bar{\mathbf{k}}$. The discrete Ricci flow is the negative gradient flow of this energy, and it converges to the global minimum.

As in [11], the discrete surface Ricci flow method was used to solve the Yamabe equation [11] and conformally map an open boundary cortical surface to a multi-hole disk.

3 Multivariate Statistics on Deformation Tensors

3.1 Derivative Map

Suppose $\phi : S_1 \to S_2$ is a map from the surface S_1 to the surface S_2. In order to simplify the formulation, we use the isothermal coordinates of both surfaces for the arguments. Let $(u_1, v_1), (u_2, v_2)$ be the isothermal coordinates of S_1 and S_2 respectively. The Riemannian metric of S_i is represented as $\mathbf{g}_i = e^{2\lambda_i}(du_i^2 + dv_i^2), i = 1, 2$.

On the local parameters, the map ϕ can be represented as $\phi(u_1, v_1) = (\phi_1(u_1, v_1), \phi_2(u_1, v_1))$. The *derivative map* of ϕ is the linear map between the tangent spaces, $d\phi : TM(p) \to TM(\phi(p))$, induced by the map ϕ. In the local parameter domain, the derivative map is the Jacobian of ϕ,

$$d\phi = \begin{pmatrix} \frac{\partial \phi_1}{\partial u_1} & \frac{\partial \phi_1}{\partial v_1} \\ \frac{\partial \phi_2}{\partial u_1} & \frac{\partial \phi_2}{\partial v_1} \end{pmatrix}.$$

Let the position vector of S_1 be $\mathbf{r}(u_1, v_1)$. Denote the tangent vector fields as $\frac{\partial}{\partial u_1} = \frac{\partial \mathbf{r}}{\partial u_1}, \frac{\partial}{\partial v_1} = \frac{\partial \mathbf{r}}{\partial v_1}$. Because (u_1, v_1) are isothermal coordinates, $\frac{\partial}{\partial u_1}$ and $\frac{\partial}{\partial v_1}$ only differ by a rotation of $\pi/2$. Therefore, we can construct an orthonormal frame on the tangent plane on S_1 as $\{e^{-\lambda_1}\frac{\partial}{\partial u_1}, e^{-\lambda_1}\frac{\partial}{\partial v_1}\}$. Similarly, we can construct an orthonormal frame on S_2 as $\{e^{-\lambda_2}\frac{\partial}{\partial u_2}, e^{-\lambda_2}\frac{\partial}{\partial v_2}\}$.

The derivative map under the orthonormal frames is represented as

$$d\phi = e^{\lambda_2 - \lambda_1} \begin{pmatrix} \frac{\partial \phi_1}{\partial u_1} & \frac{\partial \phi_1}{\partial v_1} \\ \frac{\partial \phi_2}{\partial u_1} & \frac{\partial \phi_2}{\partial v_1} \end{pmatrix}.$$

In practice, smooth surfaces are approximated by triangle meshes. The map ϕ is approximated by a simplicial map, which maps vertices to vertices, edges to

edges and faces to faces. The derivative map $d\phi$ is approximated by the linear map from one face $[v_1, v_2, v_3]$ to another one $[w_1, w_2, w_3]$. First, we isometrically embed the triangle $[v_1, v_2, v_3]$,$[w_1, w_2, w_3]$ onto the plane $\mathbb{R}^2$, the planar coordinates of the vertices of v_i, w_j are denoted using the same symbol v_i, w_j. Then we explicitly compute the linear matrix for the derivative map $d\phi$,

$$d\phi = [w_3 - w_1, w_2 - w_1][v_3 - v_1, v_2 - v_1]^{-1}.$$

In our work, we use multivariate statistics on deformation tensors [19], but adapt the concept to surface tensors. Let J be the derivative map and define the deformation tensors as $S = (J^T J)^{1/2}$. Instead of analyzing shape change based on the eigenvalues of the deformation tensor, we consider a new family of metrics, the "Log-Euclidean metrics" [18]. These metrics make computations on tensors easier to perform, as they are chosen such that the transformed values form a vector space, and statistical parameters can then be computed easily using standard formulae for Euclidean spaces.

We apply Hotelling's T^2 test on the log-Euclidean space of the deformation tensors. Given two groups of n-dimensional vectors S_i, $i = 1, ..., p$, T_j, $j = 1, ..., q$, we use the Mahalanobis distance M to measure the group mean difference,

$$M = (log\bar{S} - log\bar{T})\Sigma^{-1}(log\bar{S} - log\bar{T})$$

where $\bar{S}$ and $\bar{T}$ are the means of the two groups and Σ is the combined covariance matrix of the two groups.

4 Experimental Results

We tested our algorithm on brain anatomic surfaces extracted from 3D MRI scans of a group of 21 WS individuals and a group of 21 healthy control subjects. The cerebral cortex and landmark data are the same ones used in [20]. We tested our algorithm with different landmark sets. The first set included four selected landmark curves per hemisphere: the Central Sulcus, Superior Temporal Sulcus, Primary Intermediate Sulcus and Middle Frontal Control Line. A second set of constraint curves included seven selected landmark curves (the three new landmarks are the Precentral Sulcus, Paracentral Sulcus and Subparietal Sulcus). After we cut a cortical surface open along the selected landmark curves, the cortical surface becomes topologically equivalent to an open boundary genus 3 (4 landmarks) or genus 6 (7 landmarks) surface. So the cortical surface can be conformally mapped to a multi-hole disks with 4 and 7 boundaries, respectively. Examples of cortical surfaces with landmark curves overlaid (after cuts introduced) and their parameterization results are shown in Figure 3.

Because of the shape difference between different cortices, the centers and the radii of the inner circles are different. By computing a constrained harmonic map from each individual conformal map to a canonical multi-hole disk in the parameter domain, we can easily compute a direct surface correspondence between each of the cortical surfaces [11]. Currently, the reference canonical multi-hole disk

is arbitrarily chosen. For landmark curve matching, we guaranteed the matching of both curve ends. For other parts, we match curves based on unit speed parameterization on both curves.

Based on the surface matching results, the Jacobian matrices were computed as described in Section 3. For each point on the cortical surface, we ran permutation test with 5000 random assignments of subjects to groups to estimate the statistical significance of the areas with group differences in surface morphometry. Figure 4 and 5 illustrates our experimental results. We compared left and right cortical surface morphology between 21 control subjects and 21 WS patients with mappings constrained by a total of 4 and 7 selected landmark curves. Different sets of landmarks were used as anchors to evaluate the impact of the choice of anatomical constraints on the results. The significance maps, for the left and right hemispheres, show group differences at the voxel level, between WS patients and control subjects. Mappings with 4 and 7 selected landmark curves were computed. We detected few significant shape differences between left and right cortical surfaces (i.e., anatomical asymmetries) in both the control group and the WS group. Even so, we did find significant shape differences for both left and right cortical surfaces between WS and control subjects. We also found the regions with differences detected at the voxel level were consistent for the mappings computed with 4 and 7 selected landmark curves. However, detection power was not as high as expected in regions around the landmarks. Our future research will examine the statistics in the vicinity of the chosen landmarks, and multiple comparison correction methods, for example based on controlling the false discovery rate, will be used to assess the overall significance of the group differences.

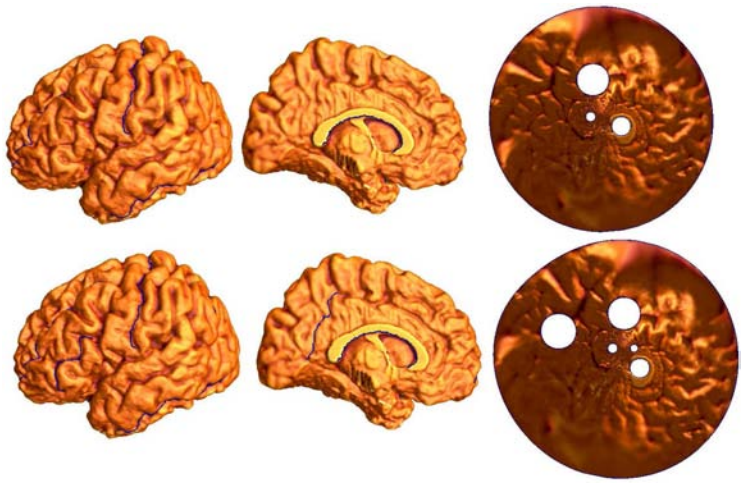

Fig. 3. Cortical surfaces with landmark curves and their conformal parameterization results. The first row shows a cortex with 4 landmarks and the second row shows a cortex with 7 landmarks (one landmark is not visible in this view).

5 Conclusions and Future Work

We applied the Ricci flow conformal parameterization for brain cortical surface registration. Based on the derivative map between two matching surfaces, a multivariate statistic on the Jacobian matrices was used to study surface morphometry in WS. Experimental results suggest that the significantly different areas were consistent with respect to the choice of landmark constraints and the algorithm has the potential to detect systematic surface abnormalities associated with disease. In the future, we will further study other possible statistics on the Jacobian matrices and find the optimal statistics for analyzing deformations computed using our Ricci flow conformal parameterization-based surface matching method. We will also validate our algorithm on larger databases of anatomical models.

References

1. Fischl, B., Sereno, M.I., Tootell, R.B., Dale, A.M.: High-resolution inter-subject averaging and a coordinate system for the cortical surface. In: Human Brain Mapping. Volume 8. (1999) 272–84
2. Bakircioglu, M., Joshi, S., Miller, M.: Landmark matching on brain surfaces via large deformation diffeomorphisms on the sphere. In: SPIE Medical Imaging. Volume 3661. (1999) 710–15
3. Leow, A., Yu, C.L., Lee, S.J., Huang, S.C., Nicolson, R., Hayashi, K.M., Protas, H., Toga, A.W., Thompson, P.M.: Brain structural mapping using a novel hybrid implicit/explicit framework based on the level-set method. NeuroImage **24**(3) (2005) 910–27
4. Thompson, P.M., Giedd, J.N., Woods, R.P., MacDonald, D., Evans, A.C., Toga, A.W.: Growth patterns in the developing human brain detected using continuum-mechanical tensor mapping. Nature **404**(6774) (March 2000) 190–193
5. Davatzikos, C.: Spatial normalization of 3D brain images using deformable models. J. Comp. Assisted Tomography **20**(4) (1996) 656–65
6. Durrleman, S., Pennec, X., Trouve, A., Thompson, P.M., Ayache, N.: Inferring brain variability from diffeomorphic deformations of currents: An integrative approach. Medical Image Analysis (2008) In Press.
7. Wang, Y., Chiang, M.C., Thompson, P.M.: Automated surface matching using mutual information applied to riemann surface structures. In: Med. Image Comp. Comput.-Assist. Intervention, Proceedings, Part II. (Oct. 2005) 666–674
8. Pitiot, A., Delingette, H., Toga, A.W., Thompson, P.M.: Learning object correspondences with the observed transport shape measure. In: IPMI. (2003) 25–37
9. Davies, R.H., Twining, C.J., Cootes, T.F., Waterton, J.C., Taylor, C.J.: A minimum description length approach to statistical shape modeling. In: IEEE TMI. Volume 21. (2002) 525–37
10. Thodberg, H.H.: Minimum description length shape and appearance models. In: IPMI. (2003) 51–62
11. Wang, Y., Gu, X., Chan, T.F., Thompson, P.M., Yau, S.T.: Brain surface conformal parameterization with the Ricci flow. In: IEEE ISBI. (2007) 1312–1315
12. Hurdal, M.K., Stephenson, K.: Cortical cartography using the discrete conformal approach of circle packings. NeuroImage **23** (2004) S119–S128

13. Angenent, S., Haker, S., Tannenbaum, A., Kikinis, R.: Conformal geometry and brain flattening. Med. Image Comput. Comput.-Assist. Intervention (Sep. 1999) 271–278
14. Gu, X., Wang, Y., Chan, T.F., Thompson, P.M., Yau, S.T.: Genus zero surface conformal mapping and its application to brain surface mapping. IEEE TMI **23**(8) (Aug. 2004) 949–958
15. Wang, Y., Lui, L.M., Gu, X., Hayashi, K.M., Chan, T.F., Toga, A.W., Thompson, P.M., Yau, S.T.: Brain surface conformal parameterization using Riemann surface structure. IEEE TMI **26**(6) (June 2007) 853–865
16. Commowick, O., Stefanescu, R., Fillard, P., Arsigny, V., Ayache, N., Pennec, X., g. Malandain: Incorporating statistical measures of anatomical variability in atlas-to-subject registration for conformal brain radiotherapy. In: MICCAI. Volume II., Palm Springs, CA, USA (2005) 927–934
17. Pennec, X., stefanescu, R., Arsigny, V., Fillard, P., Ayache, N.: Riemannian elasticity: A statistical regularization framework for non-linear registration. In: MICCAI. Volume II., Palm Springs, CA, USA (2005) 943–950
18. Arsigny, V., Fillard, P., Pennec, X., Ayache, N.: Log-Euclidean metrics for fast and simple calculus on diffusion tensors". In: Magn. Reson. Med. Volume 56. (2006) 411–421
19. Lepore, N., Brun, C., Chou, Y.Y., Chiang, M.C., Dutton, R.A., Hayashi, K.M., Luders, E., Lopez, O.L., Aizenstein, H.J., Toga, A.W., Becker, J.T., Thompson, P.M.: Generalized tensor-based morphometry of HIV/AIDS using multivariate statistics on deformation tensors. IEEE TMI **27**(1) (Jan. 2008) 129–141
20. Thompson, P.M., Lee, A.D., Dutton, R.A., Geaga, J.A., Hayashi, K.M., Eckert, M.A., Bellugi, U., Galaburda, A.M., Korenberg, J.R., Mills, D.L., Toga, A.W., Reiss, A.L.: Abnormal cortical complexity and thickness profiles mapped in Williams syndrome. J. Neurosciende (2005) 4146–4158
21. Guggenheimer, H.W.: Differential Geometry. Dover Publications (1977)
22. Hamilton, R.S.: The Ricci flow on surfaces. Mathematics and general relativity (Santa Cruz, CA, 1986), Contemp. Math. Amer.Math.Soc. Providence, RI **71** (1988)
23. Chow, B.: The Ricci flow on the 2-sphere. J. Differential Geom. **33**(2) (1991) 325–334
24. Thurston, W.P.: Geometry and Topology of Three-Manifolds. Princeton lecture notes (1976)
25. Weitraub, S.H.: Differential Forms: A Complement to Vector Calculus. Academic Press (2007)
26. Chow, B., Luo, F.: Combinatorial Ricci flows on surfaces. Journal Differential Geometry **63**(1) (2003) 97–129

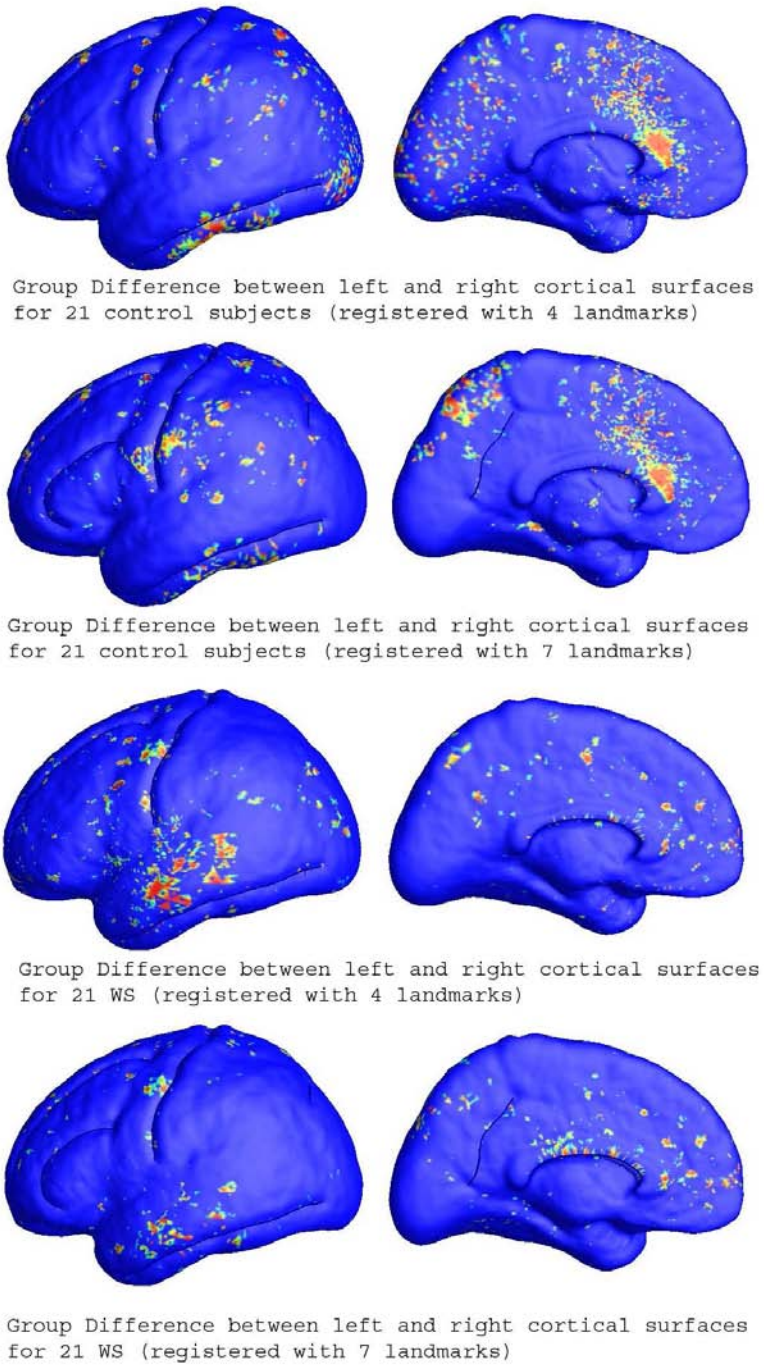

Fig. 4. Brain morphology study in 21 Williams Syndrome patients and 21 matched control subjects (intra group study).

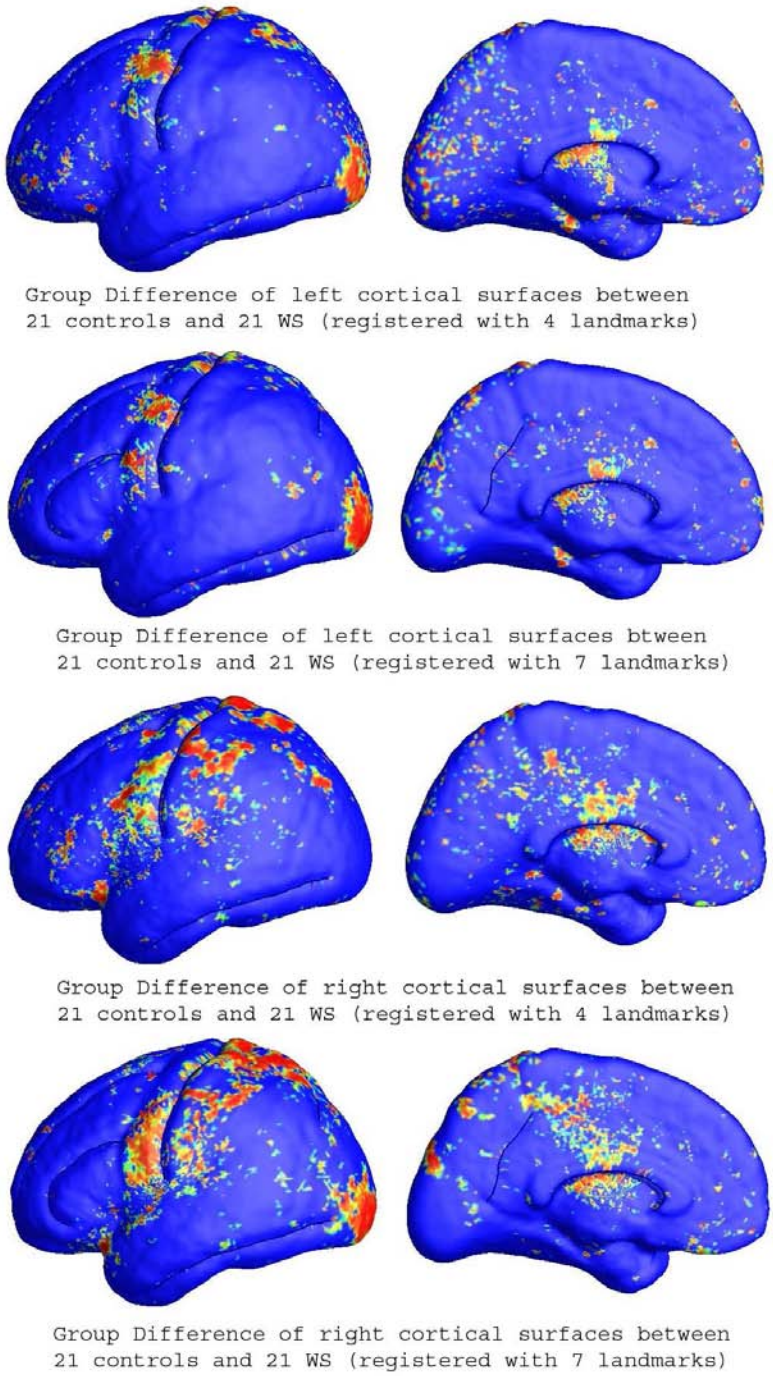

Fig. 5. Brain morphology study in 21 Williams Syndrome patients and 21 matched control subjects (inter group study).